Jul 5th, 12:00 AM - Jul 8th, 12:00 AM

Experimental and Numerical Analysis of the Hydraulic Jump Stilling Basin and the Downstream Scour Depth

L. J. Miranda
Universidad Nacional de Ingeniería, lmirandam@uni.pe

R. Sánchez
Universidad Andina del Cusco, redysanchez20@gmail.com

Experimental and Numerical Analysis of the Hydraulic Jump Stilling Basin and the Downstream Scour Depth

L.J. Miranda[1] and R. Sánchez[2]
[1]School of Civil Engineering, Universidad Nacional de Ingeniería
Lima, Túpac Amaru 210
E-mail: lmirandam@uni.pe
[2]School of Civil Engineering, Universidad Andina del Cusco
Cusco, El Sol 3107
E-mail: redysanchez20@gmail.com
PERÚ

Abstract: *This paper presents a study of a tridimensional low-head hydraulic jump stilling basin by using both physical and numerical models. Laboratory tests up to 15 hours in duration were carried out in a 1.9 m wide and 14 m long flume. Four gates produced a jet with a submerged hydraulic jump in a positive-step stilling basin, after which scour developed in a nearly uniform sand bed. Acoustic Doppler Velocimeter, piezometers and image processing were used to collect the hydrodynamic data, and Reynolds Averaged Navier-Stokes simulations developed in OpenFOAM were tested for validation purposes. Then, the study focused on (1) the temporal evolution of the experimental scour depth downstream the stilling basin and (2) the efficiency of the numerical models to reproduce the interior fields. Regarding the first point, it was found that temporal scour evolution agrees with empirical dimensionless formulation, but differences in magnitude were found, indicating that some variables should be further investigated. The validation of numerical models has shown that the K-Epsilon Standard model is much better than the K-Omega SST counterpart in reproducing velocity fields but similar values were found for turbulent kinetic energy. Pressure fluctuations numerical coefficient also showed values similar to those found by other authors, however lateral flow and Reynolds stress issues appeared because of the tridimensional nature of the case study.*

Keywords: *Hydraulic jump, stilling basin, scour, numerical model, OpenFOAM.*

1. INTRODUCTION

Energy dissipators serve to protect the riverbed and banks from erosion as well as guarantee that the hydraulic structure (dams and intakes) and other elements do not have damage because of the high turbulence flow (Khatsuria, 2004). The stilling basin is the most common dissipation structure, which uses the hydraulic jump to reduce the energy head. However, studying the flow in these stilling basins is still complex and difficult to analyse because this is an unsteady and highly turbulent flow subjected to random fluctuations (Lopardo and Romagnoli, 2009).

Understanding this phenomenon, in which macro pressure and velocity fluctuations, flow separation, eddies, and phases-mixture can be combined, is of vital importance, since they can generate vibration, fatigue and cavitation in structures (Lopardo, 1985). Likewise, the remaining energy at the outlet of the structures can scour the river bed and endanger their stability (Adduce and Sciortino, 2006).

Since the first known study of turbulence in hydraulic jumps (Rouse et al., 1959), quite a lot of studies have been carried out. In this sense, Peterka (1984) and Hager (1992) managed to compile several experiments and present a characterization and analysis of different types of hydraulic jump in energy dissipation structures. Particularly, other authors have focused on interior hydrodynamics and the air concentration in the jump (Rajaratnam, 1967) and pressure fluctuations (Lopardo, 1985; Steinke et al., 2021), among other aspects.

On the other hand, in order to obtain empirical formulas that make it possible to predict erosion downstream of hydraulic structures, researchers have conducted experiments on moving bed models with non-cohesive sand. Among these, Chatterjee et al. (1994), Hassan and Narayanan (1985) and Breusers (1967) analysed the effect of a jet that is directed from a rigid bed towards a sand bed. Subsequent investigations inquired about the downstream effect of stilling basin, and found that a

positive step affects the magnitude of the erosion depth (Oliveto and Comuniello, 2009) and this effect is highly dependent on the particle Froude number (Aminpour and Farhoudi, 2017).

Although experimentation provides real values that improve the understanding of hydrodynamics and sediment transport to propose solutions for the operation of hydraulic structures (Chanson, 2015), it has a limited scope in data collection. To address these shortcomings, Computational Fluid Dynamics (CFD) has been applied using numerical models (Bayón, 2017). In this line, turbulence modelling is not only a key aspect of CFD applications, but indispensable to study the performance in a stilling basin (Macián, 2019).

In recent years, the k-epsilon turbulence model is one of the most studied models to reproduce hydraulic jumps, and promising results have been obtained when evaluating its effectiveness in terms of water levels and velocity range, among other parameters. The numerical approach has also been used to evaluate design alternatives in terms of energy dissipation, such as the effect of converging walls (Babaali et al., 2015) or composite dissipative pools (Zhou and Wang, 2019). However, accuracy issues have been found in the estimation of the bed shear stresses (Carvalho et al., 2008) and the aeration within the hydraulic jump (Macián, 2019).

The objective of this paper is to describe the scour depth downstream the stilling basin and compare two numerical models' efficiency to predict the hydrodynamic fields. To achieve this goal, a battery of tests similar to those performed by Oliveto and Comuniello (2009) were carried out on a physical scaled model of a mobile barrage of a diversion dam. In order to complement these studies, numerical simulations with RANS approach were accomplished using the k-epsilon Standard and k-omega SST turbulence models already applied by Bayón and López (2015) for hydraulic jump stilling basin in OpenFOAM. However, the case presented here is a completely three dimensional layout, regarding water depth, velocity field, pressure, and Reynolds stresses.

2. MATERIALS AND METHODS

2.1. Experimental setup

Figure 1 shows a diagram of the flume where 5 tests were carried out under gate operating conditions (extreme flows were not studied). The mobile barrage was made up of 4 gates, two gates of 0.50 m in the middle and two gates of 0.25 m on both sides of the flume. The energy dissipator was 2.51 m long and B = 1.90 m wide. The discharge (m^3/s) was measured in a calibrated rectangular weir where a Neyrpic point gauge was installed with a precision of ± 0.2 l/s. The gate openings were established in such a way that the inlet flow depth y_0 = 0.32 m was set constant for water harvesting purposes, while the downstream levels h_{tw} (see Table 1) were controlled by an adjustable gate according to the normal depth of the river. Downstream the structure, mobile horizontal sand bed (d_{50} = 0.24 mm, d_{90} = 0.58 mm) was uniformly compacted and saturated for each test. Kinematic viscosity ν changed according the measured temperature in the day of the tests.

Table 1. Summary of the main parameters

Parameter		**Test 1**	**Test 2**	**Test 3**	**Test 4**	**Test 5**
Gate opening	a (m)	0.0259	0.0454	0.0682	0.0948	0.1289
Discharge	Q (m^3/s)	0.0634	0.1053	0.1482	0.1896	0.2327
Kinematic viscosity	ν (10^{-6} m^2/s)	1.0	0.99	0.977	0.868	0.886
Inlet velocity	U_0 (m/s)	0.1043	0.1735	0.2427	0.3111	0.3891
Shear velocity*	u^* (m/s)		0.01	0.01224	0.01414	
Froude (after gate)	Fr (-)	3.84	4.18	3.47	3.00	2.66
Particle Froude number	F_d (-)	5.46	7.39	7.63	8.21	9.67
Outlet depth	h_{tw} (m)	0.0926	0.1232	0.1478	0.1865	0.211
Characteristic erosion time	$t*$ (h)	4.37	3	1.67	1.15	0.77

**Characteristic shear velocity u* came from numerical model simulated only for tests 2, 3 and 4.*

Vectrino Acoustic Doppler Velocimeter (ADV) allowed measuring instantaneous velocity, using a sampling frequency of 50 Hz (as high as possible to allow acoustic signals to travel between bubbles that may exist in the flow) and 30 mm of sampling height to capture the smallest possible turbulent eddies flowing through the volume in intervals of 12 s. Signal to Noise Ratio (SNR) was above 30 dB, and turbulence quantities were obtained by data processing. The maximum scour was determined by taking pictures every 10 min (ranging from 8 to 15 hours) using a camera with 4160x3120 pixels located on the left side where there were three acrylic window whereas mean pressures were measure with 28 piezometers conveniently distributed throughout the stilling basin.

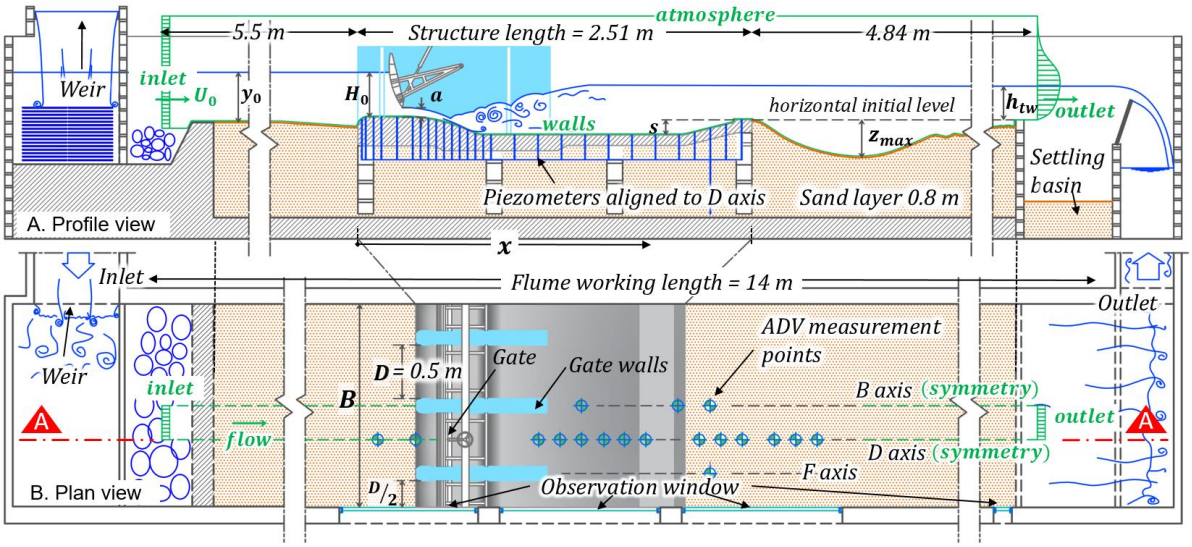

Figure 1 – Profile (A) and Plan (B) view of the physical model on experimental flume in National Laboratory of Hydraulics and numerical model boundaries (green lines).

2.2. Modelling equations

Reynolds-averaged Navier Stokes' (RANS) three-dimensional equations were used as implemented in OpenFOAM. In RANS momentum equation (1), U,p,u',ρ and F_b stand for velocity (m/s), pressure (Pa), velocity fluctuation (m/s), fluid density (Kg/m^3) and the force over the cell (m/s^2) respectively, and the symbols <> represent the time averaging operator.

$$\frac{\partial\langle\vec{U}\rangle}{\partial t} + \overrightarrow{\langle U\rangle}\nabla\cdot\overrightarrow{\langle U\rangle} = \frac{-1}{\rho}\nabla\langle p\rangle + \nu\nabla^2\overrightarrow{\langle U\rangle} + \frac{1}{\rho}\nabla\langle -\rho u'u'\rangle + \overrightarrow{F_b} \qquad (1)$$

The surface was tracked by the Volume of Fluid (VOF) method, which introduces a fluid fraction variable α_w (dimensionless) that lies between 0 and 1, calculated with the continuity flow equation (2).

$$\frac{\partial\alpha_w}{\partial t} + \nabla\cdot\left(\overrightarrow{\langle U\rangle}\alpha_w\right) = 0 \qquad (2)$$

In high turbulent flows, turbulent kinetic energy (TKE, m^2/s^2) is an important analysed variable, which is defined from velocity fluctuations in the three directions u', v' y w':

$$k = \frac{\langle u'^2\rangle + \langle v'^2\rangle + \langle w'^2\rangle}{2} \qquad (3)$$

In order to estimate the TKE and model the nonlinear terms <-$\rho u'u'$> in equation (1) that result from averaging the variables, turbulence models were used. Although some authors have used the K-Epsilon RNG model to study hydraulic jumps, Bayón (2017) found slight advantages in time consumption for the Standard version. At this stage, the K-Epsilon Standard (Launder and Spalding, 1974) and K-Omega SST (Menter et al., 2003) models were used, regarding the standard coefficients implemented in OpenFOAM 2.4. To do so, laboratory test 1 was discarded due to differences in the opening of the

gates, and also test 5 was, due to lack of bathymetry of the bed. In this way, simulations were made for three conditions, which will be called N2, N3 and N4 onwards. The PISO algorithm, created for transient flows, was used, and a Courant limit of 2 was maintained (Courant decreases from gate to jump body).

2.3. Mesh

A structured mesh comprising the inlet bed domains, gate, stilling basin, and eroded bed was constructed with the help of OpenFOAM's SnappyHexMesh application. To reproduce the high air mixture that occurs into the hydraulic jump, a higher refinement was generated in this area guaranteeing the quality of the mesh, with limits of orthogonality less than 70° and obliquity less than 4. Each mesh reached around 6 million cells.

Dimensionless cell size $\Delta x^+ = \Delta x \cdot u^*/\nu$ and time interval $\Delta t^+ = \Delta t \cdot u^{*2}/\nu$ were calculated in terms of the characteristic shear velocity *u** and the kinematic viscosity ν. The cell size was distributed over a wide range $10 < \Delta x^+ < 570$, and average time interval reached $\Delta t^+ = 0.37$. Dimensionless wall distance $y^+ = u_t \cdot y/\nu$, calculated in function of the wall shear stress u_t and the cell distance to the wall y, reached $30 < y^+ < 220$ for the stilling basin; however, for the sand bed it was $5 < y^+ < 50$.

2.4. Boundary conditions

Boundary conditions were established as suggested by Bayón (2017), considering the air and water inlets, atmosphere and walls; except for the outlet condition, for which a mixed condition (Dirichlet and Von Newman) was used, using an OpenFOAM application. *D* and *B* axis (see Figure 1) were set up as symmetry planes to simplify the study. Wall functions were assigned according to the logarithmic-law of the wall, which includes a correction for rough wall cases. A nutkRoughWallFunction was used, where the total roughness parameter *Ks* = 0.00024 (m) was assigned for the sand bed and *Ks* = 0.0001 for the concrete wall, whereas nutkWallFunction was assigned to plexiglass gate and smooth wood walls.

3. SCOUR ANALYSIS

Breusers (1967) proposed equation (4) for the maximum erosion Z_{max} at a specific time *t*.

$$\frac{z_{max}}{z_*} = \left(\frac{t}{t_*}\right)^{0.38} \qquad (4)$$

where Z_* is the characteristic length and t_* is characteristic time (see Table 1) when $Z_{max} = Z_*$. However, Oliveto and Comuniello (2009) found a better fit using an exponent of 0.19. The aforementioned authors defined Z_* based on the geometric layout of their models; but, in the present study $Z_* = H_0/2$ is used because it represents better the energy load with a potential to generate erosion in the channel. In this study, temporal evolution of the scour hole was monitored through the observation window as it is shown in Figure 2, where the maximum scour hole present quasi-homothetic evolution, similar to what was found by Bombardelli et al (2018). However, the scour depth grew faster than its location in x direction.

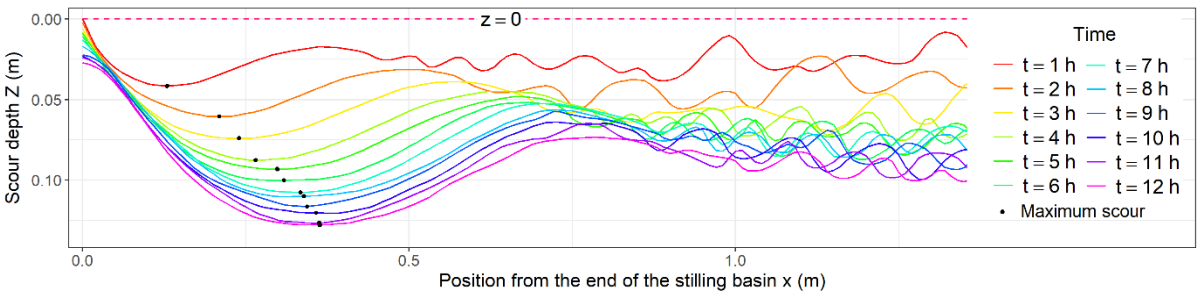

Figure 2 – Evolution of longitudinal profile for test N°2 from the observation window.

A comparison was made between the results obtained in the laboratory and the erosion calculated with

equation (5) proposed by Oliveto and Comuniello (2009), where s is end-sill height, h_{tw} is the tail water depth, $F_d = V/(g' \cdot d_{50})^{1/2}$, is the particle Froude number, $g' = g(\rho_s - \rho)/\rho$ is the modified gravity acceleration, g = gravity acceleration and ρ = density of water, ρ_s = density of sand grain, and dimensionless time $T = (g' \cdot d_{50})^{1/2} \cdot t/s$.

$$\frac{z_{max}}{s} = 3.4\left(\frac{h_{tw}}{s}\right)^{3/4}\left(\frac{d_{50}}{s}\right)^{6/5}(F_d - 1)^{6/5}T^{1/4} \qquad (5)$$

In Figure 3a, three exponential adjustments between erosion and the time scales are represented for values of $Z_{max}/Z_* < 1.5$. Figure 3a shows that the best fitting corresponds to the exponent 0.38 (Eq. 4). Figure 3b shows that experimental results were about 380% (on average) of those calculated with equation (5) at times *t = 6, 9 and 12 hours*. It could be mentioned here that the quantity z_{max}/s might not be the best way to define the non-dimensional scour since z_{max} and s are not physically related. It also should be noted that the slope of the end-sill of the physical model was 1v:4h, in contrast to the 1v:1h used by Oliveto and Comuniello (2009). As this parameter influences the scour depth (Farhoudi and Shayan, 2014), and it is not considered in the above equation, it could be another cause of difference and should be further investigated.

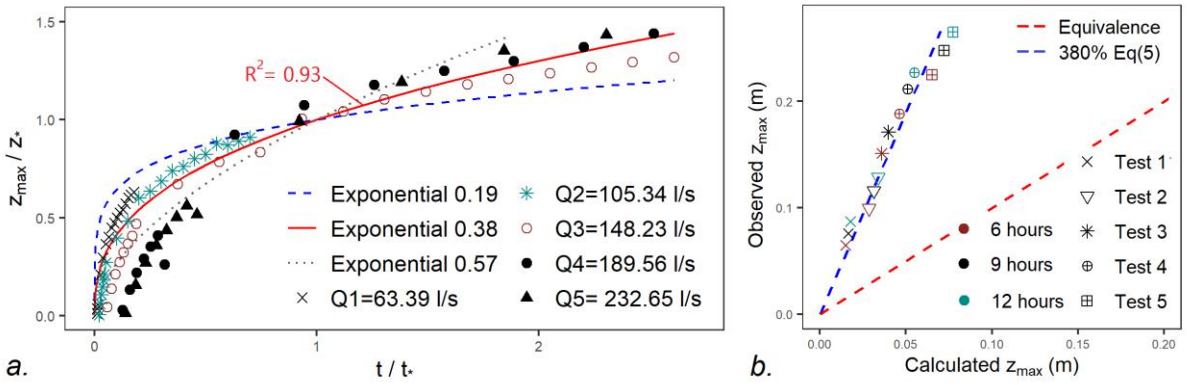

Figure 3 - (a) Dimensionless scour depth vs time and (b) observed vs calculated scour from Eq. 5.

4. VALIDATION OF RANS SIMULATIONS

Nash-Sutcliffe efficiency indicator (NSE) was used as defined by Nash and Sutcliffe (1970), where very good values from 0.75 are considered, whereas negative ones indicate that error is greater than the standard deviation. In order to determine the accuracy of the numerical model in relation to the experimental data, NSE was calculated for different quantities (Table 2).

Table 2. NSE between numerical and experimental values for different variables

Model	Case	Pressure	Water depth	TKE	Velocity profiles U_x		
					Upstream	Basin	Scour hole
k-ε	N2	0.876	-0.1868	0.889	0.801	-2.109	0.940
k-ε	N3	0.925	0.7748	0.884	0.733	-0.309	0.946
k-ε	N4	0.936	0.7948	0.978	0.769	-0.135	0.915
k-ω	N2	0.728	0.3698	0.744	0.787	-8.241	-1.839
k-ω	N3	0.915	0.7999	0.822	0.365	-3.991	-0.441
k-ω	N4	0.897	-0.2486	0.972	0.667	-1.637	-0.294

4.1. Water depth and pressure in stilling basin

During the simulation it was observed that the jump was slightly submerged in the gate, while in experiments, submergence occurs after the gate. This causes the numerical water depths to differ from experiments at the beginning of the jump. The k-ε Standard and k-ω SST models showed good accuracy

for mean pressures inside the stilling basin and, although the water depths are qualitatively similar to the observed ones (Figure 4a), the longitudinal range of measurement was small due to the limitation of the observation window, causing the NSE to reach negative values (Table 2).

The pressure fluctuations coefficient *C'p*, an important parameter to study cavitation risk (Lopardo, 1985), is calculated from numerical model and plotted in Figure 4b against the dimensionless distance x/h_1, where h_1 is the critical depth at the jump toe and *x* is the distance from this point. *C'p* values at the beginning of the jump are of the same order of magnitude as those presented by other authors, and it can be seen particularly that the estimations of *C'p* are higher in the k-ε model than in the k-ω model, except for *Fr* = 3.0. As expected for RANS type models, *C'p* drastically decreases towards the jump body, where the fluid fraction variations are minimum.

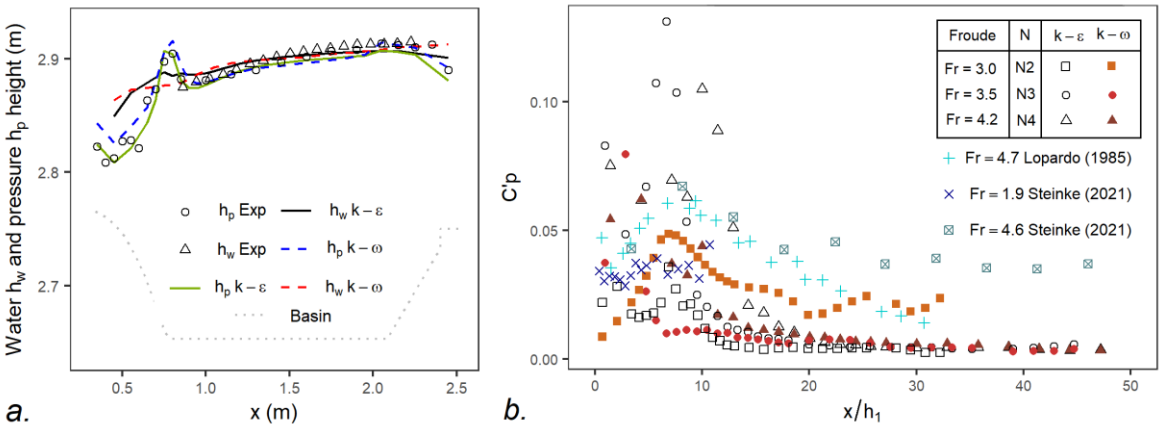

Figure 4 - (a) Water and pressure height for the test N3, and (b) numerical pressure fluctuation coefficient C'p compared with experimental results from Steinke et al. (1990) and Lopardo (1985).

4.2. Velocity, Reynolds stresses and turbulent kinetic energy

Figure 5a,b shows the velocity (u and w) before the gate (1,2), into the stilling basin (*3,4*), and the scour hole (*5,6*) for the test N3. It is observed that both Standard k-ε and k-ω SST did reproduce the velocity in the region before the gate, but problems arise later. At *x* = 1.55, the k-ε model shows positive and negative estimation errors in the *D* and *B* axis respectively, which implies a little overestimation of the lateral flow at the end of the gate wall (*x* = 1.23) or before (ADV does not capture well this region), although this error dissipates in the scour hole. On the other hand, the k-ω SST model increases this error from the hydraulic jump towards the sand bed, which may be due to a wrong reproduction of the vortices in the *xy* direction generated at the end of the gate wall. These problems could be sorted out by using other turbulence models. Constantinescu et al (2010) found, for instance, that DES models were "significantly more successful" in predicting the velocity distribution in the river channel.

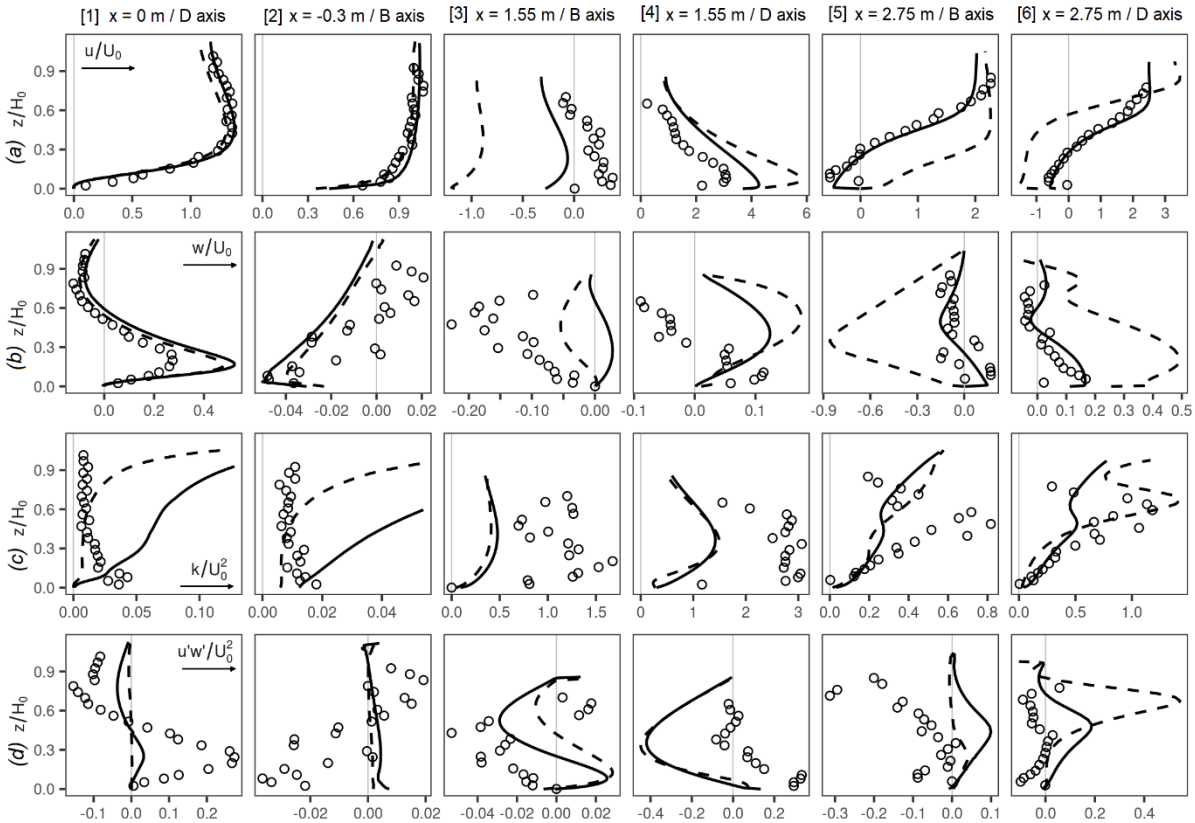

Figure 5 - Experimental (dots) and numerical k-ε (continuous) and k-ω (dashed) data for test N3.

Observed Reynolds stresses <*u'w'*> were compared using Boussinesq's approximation for numerical results without good correspondence (Figure 5d). This is possibly due to high turbulent anisotropy (in the jump region) or that sediment load (in the scour region) was not considered in the numerical model. Figure 5c also shows that numerical models overestimate the value of TKE before the gate, however underestimate that value in the interior of the hydraulic jump. This accuracy issue may be due to the jump submergence that affects the TKE production. In any case, the experimental data shows high values of TKE gradient at the stilling basin walls, so the wall functions must be further analysed. Despite these differences, the dissipation of energy was reproduced, with TKE reduction of the order of 80% from the hydraulic jump to sand bed, and the NSE taken with the logarithms of the numerical values from stilling basin to scour hole is high (Table 2).

5. CONCLUSIONS

Based on laboratory experiments and numerical simulations, it can be concluded that:

1. Unlike experiments carried out by Oliveto and Comuniello (2009), where equilibrium was reached in approximately 70 hours, the scour process was faster in the present study. Although complete equilibrium was not reached, very low scour rates were observed up to 15 hours (end of the tests) reasonably because of the difference in sand size and particle Froude number.
2. The temporal variation of the maximum erosion depth Z_{max} was measured in laboratory tests. Eq. (4) suggested by Breusers (1967) was tested and the results revealed a similarity. Then, equation (5) was compared with observed Z_{max} at the generic time t. It shows that the results obtained with equation (5) differ from those observed in experiments. The slope-height parameters should be further analysed to re-evaluate this formulation.
3. Standard k-ε and k-ω SST models were assessed and it was found that the first one reproduces the hydrodynamic fields better, having a good fit in the prediction of water levels, field velocities and kinetic energy. However, there was an error of lateral flow that generated velocity underestimation along the gate wall axis. This could be improved using a wider domain with cyclic lateral boundary condition or testing other turbulence models such as DES models.

4. It is promising that, although RANS models only capture the main characteristics, the models produced a pressure fluctuations coefficient *C'p* comparable to those obtained from other researchers, at least, in the regions with high fluid fraction variation. It can be suggested to continue studying this parameter with similar approaches.
5. Both Standard k-ε and k-ω SST models fail to correctly reproduce Reynolds stresses, but this could be due to the simplifications (isotropy, Boussinesq assumption) taken in the RANS models. Therefore, RSM (Reynolds Stress Model) could improve this shortcomings. Similarly, TKE shows larger gradients in the inlet bed and the stilling basin walls. Anyhow, both models reproduce the dissipation from the hydraulic jump to the sand bed.

6. ACKNOWLEDGMENTS

Authors thanks to all researchers and staff at National Laboratory Hydraulics for the facilities in the laboratory and the support for numerical modelling.

7. REFERENCES

Adduce, C. and Sciortino G. (2006), *Scour due to a horizontal turbulent jet, Numerical and experimental investigation*, Journal of Hydraulic Research, 44 (5), 663-673.

Aminpour, Y. and Farhoudi, J. (2017), *Similarity of local scour profiles downstream of stepped spillways,* International Journal of Civil Engineering, 15 (5), 763-774.

Babaali, H., Shamsai, A. and Vosoughifar, H. (2015), *Computational Modeling of the Hydraulic Jump in the Stilling Basin with Convergence Walls Using CFD Codes*, Arab Journal for Science and Engineering, 40, 381–395.

Bayón, A. and López, P.A. (2015), *Numerical Analysis of Hydraulic Jumps Using OpenFOAM*, J. Hydroinformatics, 17(4), 662–678.

Bayón, A. (2017), *Numerical Analysis of Air-water Flows in Hydraulic Structures Using Computational Fluid Dynamics (CFD)*. PhD Program in Water and Environmental Engineering, Polytechnic University of València, València.

Bombardelli, F.A., Palermo, M., and Pagliara, S. (2018), *Temporal evolution of jet induced scour depth in cohesionless granular beds and the phenomenological theory of turbulence*, Physics of Fluids, 30, 085109.

Breusers, H. N. C. (1967), *Time scale of two-dimensional local scour: in Nicht V. (Ed) Proceedings of the 12th IAHR Congress*, Vol. 3, Fort Collins,1967, pp. 275–282.

Carvalho, R.F., Lemos, C.M. and Ramos, C.M. (2008), *Numerical Computation of the Flow in Hydraulic Jump Stilling Basin*, Journal of Hydraulic Research, 46 (6), 739–752.

Chanson, H. (Ed.). (2015). *Energy dissipation in hydraulic structures*, CRC Press.

Chatterjee, S. S., Ghosh, S. N., and Chatterjee, M. (1994), *Local scour due to submerged horizontal jet*, Journal of Hydraulic Engineering, 1208, 973–992.

Constantinescu, G.; Koken, M.; Zeng, J. (2010), *Simulation of flow in an open channel bend of strong curvature using Detached Eddy Simulation*, River Flow 2010, 1527–1534.

Farhoudi, J., and Shayan, H. K. (2014). *Investigation on local scour downstream of adverse stilling basins,* Ain Shams Engineering Journal, 5 (2), 361-375.

Hager, W. H. (1992), *Energy dissipators and hydraulic jump*, Springer Science + Business Media B. V., Kluwer, Dordrecht, The Netherlands.

Hassan, N. M. K. and Narayanan, R. (1985), *Local scour downstream of an apron*, Journal of Hydraulic Engineering, ASCE, 111 (11), 1371-1385.

Khatsuria, R. M. (2004), *Hydraulics of spillways and energy dissipators*, CRC Press

Launder, B.E. and Spalding, D.B. (1974), The Numerical Computation of Turbulent Flows, Computer Methods in Applied Mechanics and Engineering, 3, 269-289.

Lopardo R. A. (1985), Metodología de estimación de presiones instantáneas en cuencos amortiguadores, Anales de la Universidad de Chile, 8 (5), 437–455.

Lopardo R. A. and Romagnoli M. (2009), *Pressure and velocity fluctuations in stilling basin: Proc.16th IAHR-APD Congress and 3rd Symposium of IAHR-ISHS*, Nanjing, October 20-23, 2009, pp. 2093–2098.

Macián, J.F., García, R., Huber, B., Bayón, A. and Vallés, F.J. (2019), *Approach to the Void Fraction Distribution within a Hydraulic Jump in a Typified USBR-II Stilling Basin, E-proceedings of the 38th IAHR World Congress, Water: Connecting the World*, Panama City, September 1-6, 2019, pp. 3627-3634.

Menter, F.R., Kuntz, M. and Langtry, R. (2003), *Ten Years of Industrial Experience with the SST Turbulence Model: Turbulence,* in Hanjalic, K., Nagano, Y. and Tummers, M. *(Eds) Proceedings of the 4th International Symposium on Heat and Mass Transfer*, West Redding, 2003, pp. 625-632.

Nash, J.E., and Sutcliffe, J.V. (1970), *River flow forecasting through conceptual models: Part I. A discussion of principles*. Journal of Hydrology, 119 (3), 429-442.

Oliveto, G. and Comuniello, V. (2009), *Local Scour Downstream of Positive-Step Stilling Basins*, Journal of Hydraulic Engineering, 135 (10), 846-851.

Peterka, A. J. (1984), *Hydraulic design of stilling basins and energy dissipators*, Engineering Monograph no. 25, US Bureau of Reclamation.

Rajaratnam, N. (1967), *Hydraulic Jumps*, Department of Civil Engineering, University of Alberta, Canadá.

Rouse, H., Siao, T.T. and Nagaratnam, S. (1959), *Turbulence Characteristics of the Hydraulic Jumps*, Transactions of the American Society of Civil Engineers, ASCE, 124 (1), 926-966.

Steinke, R., Dai Prá, M., Lopardo, R.A., Marques, M.G., de Melo, J.F., Priebe, P.S., and Teixeira, E.D. (2021), *Low Froude Number Stilling Basins–Hydrodynamic Characterization*, Journal of Hydraulic Engineering, 147 (4), s.p.

Zhou, Z. and Wang, J. (2019), *Energy dissipation due to the compound stilling basin: E-proceedings of the 38th IAHR World Congress, Water: Connecting the World*. Panama City, September 1-6, 2019, pp. 3515-3524.